Solar Energy Materials & Solar Cells 260 (2023) 112451

Contents lists available at ScienceDirect

Solar Energy Materials and Solar Cells

journal homepage: www.elsevier.com/locate/solmat

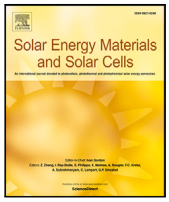

Process influences on LeTID in Ga-doped silicon

Felix Maischner [a,b,*], Wolfram Kwapil [a,b,**], Johannes M. Greulich [a], Yujin Jung [c], Hannes Höffler [a], Pierre Saint-Cast [a], Martin C. Schubert [a,b], Stefan Rein [a], Stefan W. Glunz [a,b]

[a] Fraunhofer Institute for Solar Energy Systems ISE, Freiburg, Germany
[b] Laboratory for Photovoltaic Energy Conversion, Department of Sustainable Systems Engineering (INATECH), University of Freiburg, Freiburg, Germany
[c] Institute for Energy Technology, Korea University, Seoul, Republic of Korea

ARTICLE INFO

Keywords:
LeTID
Silicon
Gallium
FFO

ABSTRACT

Light- and elevated temperature-induced degradation (LeTID), which can lead to significant module power loss in the field, has been extensively studied for boron (B)-doped silicon solar cells in the past. Current mass-production has shifted to gallium (Ga)-doped silicon substrates. Therefore, process influences on LeTID must be re-investigated for the changed acceptor species, as the LeTID-degradation extent and kinetics can be drastically different. We study the influence of the dielectric layer and the firing profile on the LeTID extent in Ga-doped lifetime samples. Furthermore, the effect of the bulk doping concentration is investigated. We find that a dielectric layer with high hydrogen content, a-SiN_x:H (PECVD), leads to largest LeTID degradation. However, AlO_x (PECVD) interlayers serve as very effective diffusion barriers, thus mitigating LeTID, as expected from studies on B-doped material. We observe no significant dependence of LeTID susceptibility on the doping concentration. Most interestingly, it appears that modifying the peak firing temperature, which has the greatest effect on the extent of LeTID in B-doped silicon, has a much smaller effect on the Ga-doped material, with LeTID being observed even when firing at 700 °C.

1. Introduction

Light and elevated temperature induced degradation (LeTID) [1] is, besides boron oxygen (BO)-degradation [2], the largest factor of degradation of boron (B)-doped passivated emitter and rear cells (PERC) in the field [3]. It has therefore been studied extensively on cells and lifetime samples made from B-doped silicon. The exact nature of the defect is still controversial. Most researchers agree that hydrogen (H), which diffuses from the passivation layers into the bulk silicon during firing, plays an important role in its formation [4–6].

To solve the problem of BO-degradation, many cell manufacturers have meanwhile changed to producing gallium (Ga)-doped cells. Some studies report that this also largely solved the LeTID-problem, since the degradation is less severe [7–10]. However, since there are indications that LeTID impacts Ga-doped silicon samples differently compared to B-doped Si, it is yet too early to reach a final judgement. For example, it was shown that at field-relevant temperatures around 75 °C, high carrier injection suppresses LeTID in Ga-doped silicon [11], which may have impacted published studies. Also, the processing and thermal history of solar cells seem to influence Ga-doped samples in an unusual way [12]. One factor that could influence the behavior of the two materials is the difference in activation energy for the formation of B–H and Ga–H bonds (B–H: 1.20 eV, Ga–H: 1.04 eV) [13]. This could lead to different concentrations of molecular and atomic hydrogen and hence different diffusion and reaction rates of the LeTID-defect formation and dissociation.

All these uncertainties in LeTID susceptibility raise the fundamental question of which processing steps and material properties influence the extent of LeTID in Ga-doped samples. In this work we take a step back and investigate in detail the influences of cell processing steps that are well established for B-doped but not for Ga-doped samples. In particular, we analyze different passivation layers typically used in the manufacturing of PERC solar cells, different fast firing conditions and samples made from silicon with different base doping concentrations. From these results we derive recommendations for LeTID suppression strategies. We also propose an accelerated test procedure that can be used to estimate the LeTID behavior of cells in less than 0.1% of the time required by a conventional test.

* Corresponding author at: Fraunhofer Institute for Solar Energy Systems ISE, Freiburg, Germany.
** Corresponding author.
E-mail addresses: felix.maischner@ise.fraunhofer.de (F. Maischner), wolfram.kwapil@ise.fraunhofer.de (W. Kwapil).

https://doi.org/10.1016/j.solmat.2023.112451
Received 23 March 2023; Received in revised form 21 June 2023; Accepted 26 June 2023
Available online 14 July 2023

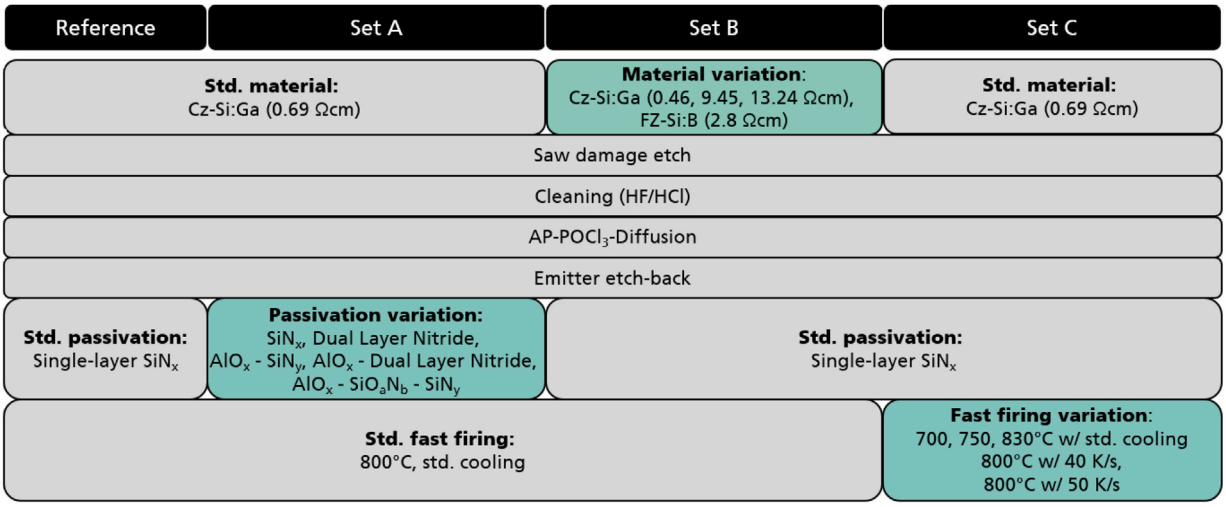

Fig. 1. Process sequence of the samples analyzed in this paper. For details on the passivation variation and fast firing variation, see Figs. 2 and 3 respectively.

2. Experimental

2.1. Lifetime sample processing

In this study, three sets of silicon samples (named set A, B and C) were produced by varying one process parameter of the reference process sequence in each set to investigate its influence on LeTID. For all variations, each group consisted of two samples. For the reference process sequence, industrial Ga-doped Czochralski (Cz)-grown Si wafers of M2 format with a base doping of 0.69 Ωcm were saw-damage-etched, cleaned, and an emitter with a sheet resistance of 83 Ω/sq. was formed in a diffusion oven based on $POCl_3$ as dopant source. It was only introduced to getter impurities and has subsequently been etched back on both sides to avoid emitter recombination. The samples were then symmetrically passivated by plasma-enhanced chemical vapor deposition (PECVD) using a c.PLASMA 2.600 from centrotherm. The layer we applied was a hydrogen-rich silicon nitride of refractive index $n = 2.05$ and a thickness of 75 nm, henceforth abbreviated to SiN_x. Afterwards the samples were fired at a measured peak temperature (T_{peak}) of 800 °C. The reference process sequence and all variations can be seen in Fig. 1.

For set A, the passivation layer was varied between five groups. For all experiments, each group consisted of two samples. The samples were all coated symmetrically using PECVD with dielectric layers, which are similar to those in an industrial PERC cell process. The reference group received the previously described SiN_x. The second passivation stack consisted of two layers of silicon nitride, first (in contact with the silicon surface) a 25 nm thick layer with $n = 2.1$ to 2.3 and second a 50 nm thick layer with $n = 2.05$. This stack will be called dual layer nitride. The third and fourth passivation stacks consisted of the two that were just described with an additional 5 nm AlO_x interlayer between the silicon wafer and the SiN_x. The last passivation we investigated was a stack of AlO_x–SiO_aN_b–SiN_y, typically used for rear surface passivation. For this stack, the thickness of the individual layers is unknown but the total thickness of it was measured to be 110 nm. To correct for the varying optical properties of samples passivated with different dielectric layers, the firing process was adapted for each group. Fig. 2 illustrates all analyzed passivation layers.

For set B, four groups with a Ga-doping variation between 0.46 Ωcm and 13.24 Ωcm were investigated using the reference process sequence. B-doped float-zone (FZ), magnetically-grown Czochralski (mCz), mono-cast Ga-doped wafers that were made with the seed manipulation for artificially controlled defects technique (SMART) [14], and conventional Cz-Si:B reference samples were processed in parallel for comparison. However, with the exception of the FZ samples, all

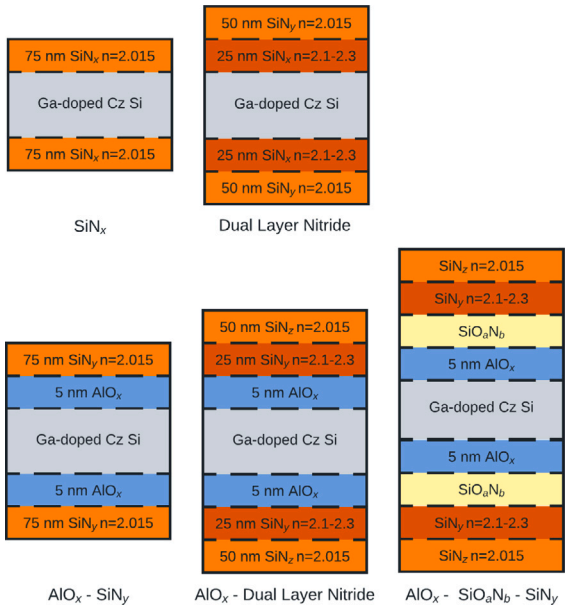

Fig. 2. Schematic of all the passivation stacks analyzed, together with the names used for them in this publication.

additional samples suffered from low initial lifetime, preventing the analysis of the normalized defect density (NDD) described below. In the case of the Cz-Si:B samples, this can be explained by BO-degradation. We therefore only discuss measurements from the FZ samples, but are open to share all data upon reasonable request.

Set C consists of six groups of 0.69 Ωcm Ga-doped wafers coated with the single SiN_x layer used in the reference process sequence. In this set, six different fast firing profiles were used, depicted in Fig. 3. T_{peak} was varied between 700 °C and 830 °C. Additionally, the cooling rate was changed between the standard rate of 81 K/s and 40 K/s at a constant peak firing temperature of 800 °C. It should be noted that decreasing the firing temperature also led to an unintentional decrease of the cooling rate in the standard firing profile (66 K/s for the sample fired at 750 °C and 57 K/s for the sample fired at 700 °C). Increasing the firing temperature to 830 °C, however, did not significantly change the cooling rate. Details on the firing process, the definition of the cooling rate and a discussion of the likely mechanism behind the LeTID suppression can be found in our previous publication [15]. In it, we also

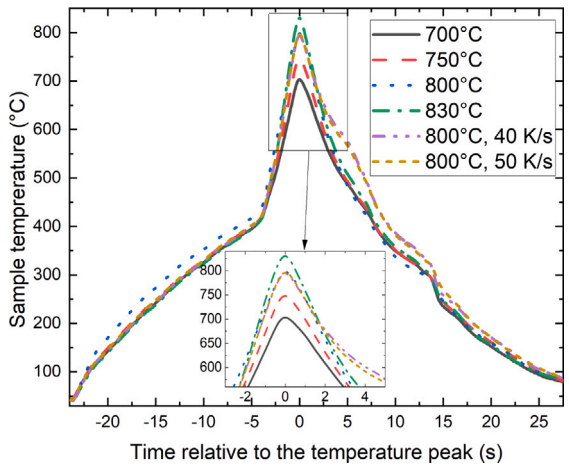

Fig. 3. Time–temperature profiles of fast-firing processes with a set peak temperature between 700 °C and 830 °C and two different cooling rates. The inset shows a magnification of the data in the region around the peak.

show that a cooling rate of 50 K/s is indeed applicable to the production of B-doped silicon PERC-cells with no significant loss in fill factor or efficiency. More recent results also show that the same is true for PERC cells made from Ga-doped silicon [16]. After firing, all sets of samples were laser-cut into quarters.

2.2. LeTID conditions

Out of each group, two quartered samples were subjected to LeTID degradation conditions at 75 °C and 0.15 suns eq. (hereafter referred to as "standard test"). Here, 1 sun eq. is defined to express an illumination intensity of 1 kW/m^2. These test conditions were first proposed by Kersten et al., intending to recreate the degradation conditions a cell would experience during 20 years in the field [17]. In addition to the standard test condition, all sets of samples were also subjected to an illumination intensity of 2 suns eq. at 140 °C, which will be labeled "accelerated test" in the following. These conditions were chosen in an attempt to balance injection and temperature influences to obtain a LeTID degradation extent comparable to the standard test, but within a significantly shorter time period. As mentioned above, we have shown in a previous publication [11] that high carrier injection drastically reduces the impact of LeTID on Ga-doped samples. The degradation that does occur, however, happens on a shorter timescale, since a higher injection leads to a higher degradation rate [7], a behavior which is also observed in B-doped silicon. On the other hand, Winter et al. [7] showed that higher temperatures not only result in accelerated LeTID degradation, but also increase the maximum defect density.

2.2.1. Carrier lifetime and NDD analysis

At increasing time intervals, the carrier lifetime was recorded using QSSPC measurements taken with a WCT-120 from Sinton Instruments during the standard test, or via modulated photoluminescence ("modPL") [18], during the accelerated test. To avoid analyzing different injection regimes in samples with different dopant concentrations N_D, all samples were analyzed at $\Delta n = \frac{N_D}{10}$.

After LeTID testing, the LeTID degradation of each sample was evaluated by calculating the NDD_{max} (in the following abbreviated to NDD) using the formula

$$NDD_{max} = \frac{1}{\tau_{min}} - \frac{1}{\tau_{max}},$$

where τ_{max} is the first lifetime maximum, which for most samples was reached at the second measurement (as explained in Section 3.1), and τ_{min} is the subsequent lifetime minimum. All values are given in ms^{-1} rounded to the first decimal place. Since we did not measure the lifetime continuously during the degradation, we most likely did not observe the actual lifetime maximum and minimum. Therefore, the calculated NDD gives a lower bound of the actual NDD.

Table 1
Initial effective lifetime at $\Delta n = \frac{N_D}{10}$ and NDD for all samples tested with the standard LeTID test. The first values of each variation represent the samples that are shown in the previous figures.

Group	τ_{max} [µs]	NDD_{max} [ms^{-1}]
Dielectric layer		
SiN_x	269 278	5.9 6.0
Dual layer nitride	312 320	3.4 2.5
AlO_x–SiN_x	207 225	0.9 0.3
AlO_x–Dual layer nitride	241 230	0.3 0.7
AlO_x–SiO_aN_b–SiN_y	241 234	0.3 0.8
Doping		
0.46 Ωcm	258 258	7.4 7.4
0.69 Ωcm	360 358	9.5 9.4
9.45 Ωcm	482 364	8.3 7.0
13.24 Ωcm	592 334	14.8 12.1
FZ:B, 2.80 Ωcm	485 476	4.4 4.3
T_{peak}		
700 °C	406 —	2.7 —
750 °C	387 395	3.7 4.7
800 °C	360 358	9.5 9.4
830 °C	354 339	5.9 5.5
Cooling rate		
81 K/s (Std.)	360 358	9.5 9.3
50 K/s	406 400	0.4 1.1
40 K/s	443 424	0.9 —

3. Results and discussion

3.1. Standard and accelerated LeTID test

Fig. 4 shows the LeTID test results of sister samples subjected to different degradation conditions, namely the standard test (a) and the accelerated test (b). It should be noted that all standard tests were performed on two quartered samples for each process variation. For clarity, only one sample from each group is shown, as no significantly different behavior was observed between two such samples. We did, however, include the data from both samples in Table 1, showing initial lifetime as well as NDD for all groups.

We observe that, at least in the present case, the accelerated test does indeed provide the same qualitative, relative information about the influence of the dielectric layer on LeTID, within well below one

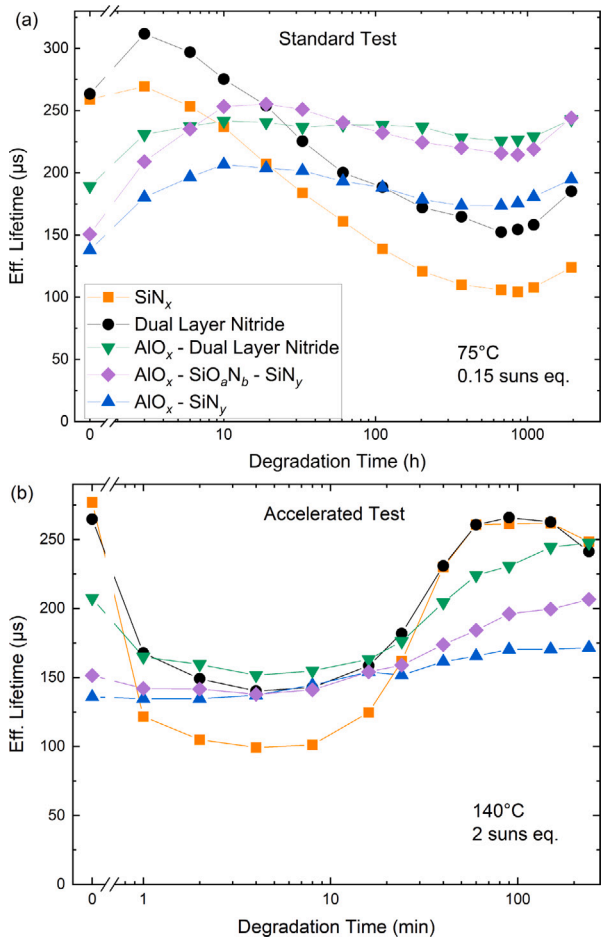

Fig. 4. Effective lifetime of differently coated Ga-doped Si wafers (0.69 Ωcm) evaluated at $\Delta n = \frac{N_D}{10}$ during application of two different degradation conditions. (a) standard test, 75 °C + 0.15 suns eq., measured via QSSPC; (b) accelerated test, 140 °C + 2 suns eq., measured via modPL. Note the different units of time on the x-axis.

thousandth of the time. In both tests, the single SiN_x layer leads to the highest LeTID susceptibility. However, during the first 10 h of the standard test, the carrier lifetime of the samples featuring an AlO_x interlayer increases before LeTID sets in. An analysis of the excess carrier density dependent lifetime (not shown here) revealed a decrease in J_{0S} over the first four measurements. This indicates that a delayed activation of the surface passivation takes place. Hamer et al. [19] have observed an initial increase of lifetime under very similar conditions (150 °C, 2 suns eq.) in B-doped silicon lifetime samples passivated with an AlO_x–SiN_y stack. They also attributed this behavior to the activation of the AlO_x:H passivation via thermal annealing. Since this effect is independent of LeTID, we chose the first lifetime maximum instead of the initial lifetime for the NDD calculation.

The initial increase of lifetime was not observed in the accelerated test. However, under these conditions the samples already strongly degrade after one minute, indicating that the temporal resolution may have been too low to observe an initial lifetime increase.

There is also a feature that can only be observed in the accelerated test: Both the SiN_x and dual layer nitride passivated samples start to degrade a second time towards the end of the test. This can most likely be explained by surface-related degradation (SRD). Although this has not yet been described in Ga-doped Cz samples, it has been previously observed on B-doped Fz [20], Cz [21,22] and mc-Si [22] samples. As in the cited literature, SRD is most prominent in samples where there is no AlO_x interlayer blocking the hydrogen diffusion from the SiN_x into the silicon bulk. Since the excess carrier density range obtained during measurements was too low to properly determine J_{0S}, we unfortunately cannot provide more insight at present. Interestingly, according to literature and our own experience, SRD seems to set in only after a complete LeTID degradation and regeneration cycle (if the sample is susceptible to LeTID). Since LeTID regeneration was not finished after the standard test, we observe SRD only in the accelerated test.

3.2. Influence of the dielectric coating

Analyzing Fig. 4(a), we observe the strongest LeTID degradation in the samples that were passivated with SiN_x only, with an NDD of 5.9–6.0 ms^{-1}, followed by the dual layer nitride (2.5–3.4 ms^{-1}). All passivation layers including an AlO_x interlayer showed similar, low NDDs between 0.3 ms^{-1} and 0.9 ms^{-1}.

The dual layer nitride was intended to increase the bulk hydrogen concentration, since the interlayer with $n = 2.1$ to 2.3 contains more hydrogen than the layer with $n = 2.05$. Therefore, we expected these samples to show stronger LeTID degradation. As reported by Chen et al. [23], SiN_x:H layers with low Si–N bond density (and hence a high refractive index) have a higher Si–H bond density after deposition compared to layers with high Si–N bond density. However, after firing, the trend is reversed as the SiN_x with low Si–N bond density loses almost all its Si–H bonds, which by contrast are stable for its counterpart with high Si–N bond density. This could explain why the dual layer nitride may introduce less hydrogen into the bulk during firing than the single SiN_x layer.

The low NDD in the samples with an AlO_x interlayer can be explained by that layer acting as a diffusion barrier, preventing hydrogen from leaving the SiN_x layers and entering the silicon bulk, thus reducing the LeTID extent. Similar observations have been made for B-doped silicon by, e.g., Schmid et al. [24]. Analyzing AlO_x interlayers of different thicknesses, they found a reduction in NDD by a factor of 2.5 for multicrystalline silicon samples and a layer thickness of 5 nm compared to the degradation without an AlO_x interlayer. Thicker layers linearly reduced the NDD further. We, on the other hand, observed NDD reductions by factors between four and ten (see Table 1).

It should be noted that Schmid et al. analyzed AlO_x layers formed by atomic layer deposition (ALD) instead of PECVD. Varshney et al. [25] found that AlO_x layers only act as diffusion barriers when deposited using ALD, and layers deposited using PECVD even increased LeTID degradation. They speculated that this is to be explained by PECVD-AlO_x containing more hydrogen than AlO_x layers deposited using ALD. They also mention that PECVD films are reported to be pinhole-rich, which might reduce their ability to block hydrogen diffusion. This seems to contradict our findings. However, this discrepancy could be due to the particular designs of the used reaction chambers: whereas Varshney et al. and their cited reference used a remote plasma (Roth & Rau MAiA) for layer deposition, our layers were deposited by a c.PLASMA 2.600 implementing a direct plasma. In literature, differences between direct and remote plasma deposited dielectrics have been reported [26]. We therefore believe that the difference between our results and those of Varshney et al. could be explained by the different types of PECVD techniques used to deposit the AlO_x layer.

3.3. Impact of doping concentration

Expecting that Ga–H pair formation strongly influences the LeTID behavior in Ga-doped samples, we investigated the doping dependence between 0.46 Ωcm and 13.24 Ωcm, shown in Fig. 5. As expected, the doping has a significant impact on the initial carrier lifetime, leading to lower lifetimes in the higher doped samples. All samples were illuminated with 0.15 suns eq. which led to a lower excess carrier density in the higher doped samples. Since the degradation and regeneration rate of LeTID depend on the excess carrier density, higher doping leads to a later onset of regeneration. Regeneration of the samples with

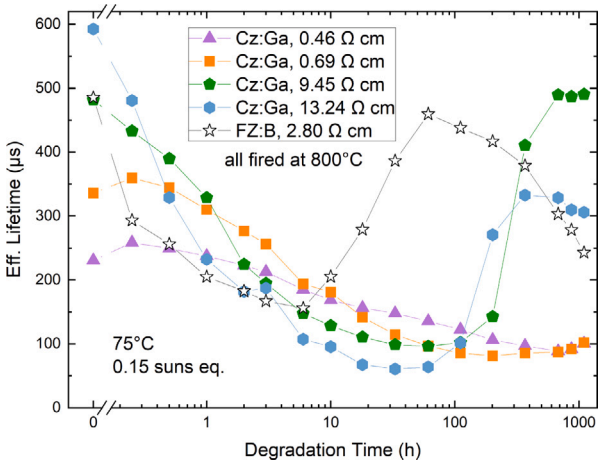

Fig. 5. Effective lifetime of Ga-doped Si wafers with varying base resistivity during standard LeTID test measured via QSSPC at $\Delta n = \frac{N_D}{10}$.

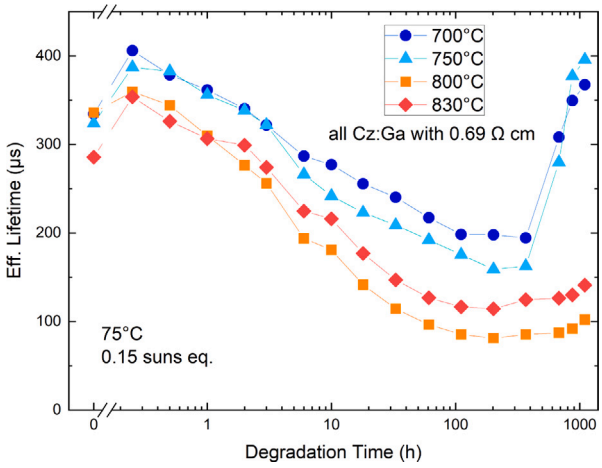

Fig. 6. Eff. lifetime of Ga-doped Si wafers (0.69 Ωcm) during standard LeTID test after firing with different T_{peak}.

resistivities of 0.46 Ωcm and 0.69 Ωcm was therefore not observed in this test. Additionally, we conducted an accelerated test with identically manufactured samples, the results of which are not shown here. In that test, we were able do observe the regeneration of all samples.

Furthermore, it is obvious that all samples degrade. There are differences in terms of normalized defect densities (see Table 1), with the lowest doped samples degrading more, but all other samples behave almost identically. Overall, doping concentration has a very limited impact on LeTID degradation when compared to that of other parameters.

When comparing the degradation of the Ga-doped samples to that of a B-doped float-zone reference sample, it can be seen that especially the timescale of the degradation is quite different. The Ga-doped samples reach the point of maximum degradation after 33 to 864 h and only two of them finish regeneration during the test after 672 to 864 h. The B-doped sample, however, reaches these two points after 6 h and 61 h respectively. This behavior was to be expected, since it has already been shown that LeTID degradation and regeneration is faster in B-doped samples [11,27].

Comparing the NDD of the samples in this variation, we find that all Ga-doped samples show a higher degradation (7.0–14.8) ms^{-1} than the B-doped FZ samples (4.3–4.4) ms^{-1}. This might to some extent be explained by the earlier onset of regeneration observed in the FZ samples, which reduces the NDD. Nevertheless, we conclude that Ga-doped samples at least do not generally degrade less than B-doped samples. This is in contrast to many previous studies, as mentioned in Section 1.

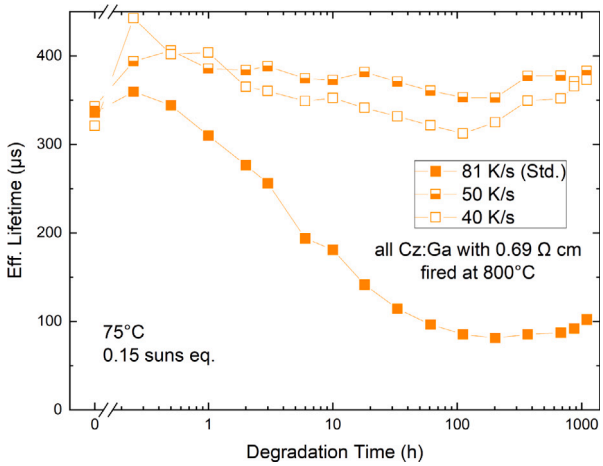

Fig. 7. Effective lifetime of Ga-doped Si wafers (0.69 Ωcm) during standard LeTID test after firing at T_{peak} = 800 °C with different cooling rates.

While the late onset of regeneration in Ga-doped samples may in part be caused by the lower initial lifetime, leading to a lower excess carrier density during illumination, we suspect that the difference in activation energy for the formation of B–H and Ga–H bonds influences this behavior as well.

3.4. Impact of firing profile

We observe only a small influence of the peak firing temperature on the LeTID extent in Ga-doped samples, with higher T_{peak} leading to increased degradation extent. This is also reflected in the NDD shown in Table 1, which increases from 2.7 ms^{-1} for a sample fired at 700 °C to 9.4–9.5 ms^{-1} for samples fired at 800 °C. Further increasing the temperature to 830 °C, however, slightly decreased the NDD to 5.5–5.9 ms^{-1}.

Surprisingly, as shown in Fig. 6, even the sample fired at T_{peak} = 700 °C degrades strongly. This observation is in strong contrast to the results obtained on B-doped material [28], where such extents of degradation were only observed in multicrystalline samples containing an AlO_x interlayer on at least one side of the sample and an emitter on the other. It is unclear what could cause this unexpected behavior.

In Fig. 7, it can be seen that decreasing the cooling rate from 81 K/s to 50 K/s significantly mitigates LeTID degradation in the tested Ga-doped lifetime samples, reducing the NDD from 9.3–9.5 ms^{-1} to 0.4–1.1 ms^{-1}. However, lowering the rate to 40 K/s does not further reduce LeTID, with an NDD of 0.9 ms^{-1}.

According to Fig. 6, the samples fired at lower peak temperatures regenerate faster and stronger than their counterparts fired at 800 °C and 830 °C. Since the regeneration rate increases with increasing excess carrier density, this difference can in part be explained by the higher carrier lifetime in the samples fired at 700 °C and 750 °C. However, as we have shown in a previous study [11], the regeneration is sensitive to lateral inhomogeneities of the carrier lifetime. Regeneration spreads out from areas with locally higher lifetime, sometimes leading to a "regeneration front" moving across the wafer area. The abrupt increase in the carrier lifetime between 368 and 672 h in the samples fired at low peak temperatures is a strong indication for such an event; apparently, this did not happen in the samples fired at higher temperatures.

4. Conclusion

In this study we showed that Ga-doped Si can be just as susceptible to LeTID as B-doped material. Careful processing is therefore required to minimize LeTID impact on longterm module performance. As is true for their B-doped counterparts, Ga-doped silicon samples show more LeTID-degradation when passivated with hydrogen-rich SiN_x layers using plasma-enhanced chemical vapor deposition (PECVD). An interlayer of AlO_x acts as a diffusion barrier, preventing hydrogen from entering the bulk, thus reducing LeTID-degradation.

Lower base doping concentrations increase the initial lifetime and, via an increased excess carrier concentration during illumination, also accelerate degradation and subsequent regeneration. However, the do not significantly affect the maximum degradation, with normalized defect density (NDD) remaining almost constant at 7.4–9.5 ms^{-1} for resistivities ranging from 0.46 Ωcm to 9.45 Ωcm and only increased to 12.1–14.8 ms^{-1} when increasing the resistivity further to 13.24 Ωcm. When compared to B-doped FZ samples, our Ga-doped samples showed stronger degradation with NDDs between 7.0 ms^{-1} to 14.8 ms^{-1} instead of 4.3–4.4 ms^{-1}.

The measured peak temperature T_{peak} has some influence on the severity of LeTID degradation, with higher temperatures (up to 800 °C) leading to stronger degradation. In contrast to previous experiments on B-doped samples, even a sample fired at 700 °C showed severe LeTID-degradation.

The method of mitigating LeTID by lowering the cooling rate during fast firing has the same effect on Ga-doped lifetime samples. Lowering the cooling rate from the standard 81 K/s to 50 K/s reduces the NDD by a factor of ten. A further decrease to 40 K/s does not result in a stronger LeTID suppression.

Thus, many of the strategies developed to reduce LeTID in B-doped samples can also be applied to Ga-doped materials. A passivation stack including an AlO_x interlayer of at least a 5 nm thickness, combined with a firing process with a slow cooling rate would likely be most effective.

Lastly, increasing illumination and temperature to 2 suns eq. and 140 °C, respectively, is a viable way to accelerate LeTID testing significantly while still obtaining meaningful results.

CRediT authorship contribution statement

Felix Maischner: Writing – original draft, Investigation, Formal analysis, Conceptualization. **Wolfram Kwapil:** Writing – original draft, Supervision, Conceptualization. **Johannes M. Greulich:** Writing – review & editing, Supervision. **Yujin Jung:** Investigation. **Hannes Höffler:** Writing – review & editing, Investigation. **Pierre Saint-Cast:** Writing – review & editing. **Martin C. Schubert:** Writing – review & editing, Project administration, Funding acquisition. **Stefan Rein:** Writing – review & editing, Project administration, Funding acquisition. **Stefan W. Glunz:** Writing – review & editing, Supervision.

Declaration of competing interest

The authors declare that they have no known competing financial interests or personal relationships that could have appeared to influence the work reported in this paper.

Data availability

Data will be made available on request

Acknowledgments

The authors acknowledge the financial support by the Federal Ministry for Economic Affairs and Climate Action of Germany in the projects GutenMorgen (project number 246895) and GagaRIn (project number 355015).

References

[1] K. Ramspeck, S. Zimmermann, H. Nagel, A. Metz, Y. Gassenbauer, B. Birkmann, A. Seidl, Light induced degradation of rear passivated mc-Si solar cells, in: Proceedings of the 27th European Photovoltaic Solar Energy Conference and Exhibition, 2012.

[2] S.W. Glunz, S. Rein, W. Warta, J. Knobloch, W. Wettling, Degradation of carrier lifetime in Cz silicon solar cells, Sol. Energy Mater. Sol. Cells 65 (1) (2001) 219–229, PVSEC 11 Part I.

[3] F. Fertig, I. Höger, M. Schaper, R. Lantzsch, F. Kersten, M. Bartzsch, F. Frühauf, B.G. Lee, A. Mette, B. Klöter, J.W. Müller, Q.antum on p-type Cz silicon: High-end performance and reliability, in: 2018 IEEE 7th World Conference on Photovoltaic Energy Conversion, (A Joint Conference of 45th IEEE PVSC, 28th PVSEC & 34th EU PVSEC), WCPEC, 2018, pp. 0993–0995.

[4] A.C.née Wenham, S. Wenham, R. Chen, C. Chan, D. Chen, B. Hallam, D. Payne, T. Fung, M. Kim, S. Liu, S. Wang, K. Kim, A. Samadi, C. Sen, C. Vargas, U. Varshney, B.V. Stefani, P. Hamer, G. Bourret-Sicotte, N. Nampalli, Z. Hameiri, C. Chong, M. Abbott, Hydrogen-induced degradation, in: 2018 IEEE 7th World Conference on Photovoltaic Energy Conversion, (A Joint Conference of 45th IEEE PVSC, 28th PVSEC & 34th EU PVSEC), WCPEC, 2018, pp. 0001–0008.

[5] M. Kim, D. Chen, M. Abbott, S. Wenham, B. Hallam, Role of hydrogen: Formation and passivation of meta-stable defects due to hydrogen in silicon, AIP Conf. Proc. 1999 (1) (2018) 130010.

[6] U. Varshney, M. Abbott, A. Ciesla, D. Chen, S. Liu, C. Sen, M. Kim, S. Wenham, B. Hoex, C. Chan, Evaluating the impact of SiN_x thickness on lifetime degradation in silicon, IEEE J. Photovolt. 9 (3) (2019) 601–607.

[7] M. Winter, D.C. Walter, B. Min, R. Peibst, R. Brendel, J. Schmidt, Light and elevated temperature induced degradation and recovery of gallium-doped Czochralski-silicon solar cells, Sci. Rep. 12 (1) (2022) 1–8.

[8] F. Kersten, R. Lantzsch, N. Buschmann, Y. Neumann, K. Petter, M. Kauert, F. Stenzel, F. Fertig, A. Schönmann, B. Faulwetter-Quandt, K. Duncker, K. Kim, E. Jarzembowski, M. Junghänel, A. Weihrauch, S. Wasmer, B. Reiche, C. Klenke, B. Lee, F. Frühauf, I. Höger, M. Schaper, J.W. Müller, D.J.W. Jeong, LeTID sensitivity of gallium- & boron-doped Cz-Si PERC solar cells with an average conversion efficiency of 23.6 %, AIP Conf. Proc. 2487 (1) (2022) 130007.

[9] C. Chen, H. Wang, J. Wang, J. Lv, H. Yang, Performance degradation of commercial Ga-doped passivated emitter and rear cell solar modules in the field, Prog. Photovolt., Res. Appl. 30 (3) (2022) 300–309.

[10] K. Petter, K. Hubener, F. Kersten, M. Bartzsch, F. Fertig, B. Klöter, J. Müller, Dependence of LeTID on brick height for different wafer suppliers with several resistivities and dopants, in: 9th Int. Work. Cryst. Silicon Sol. Cells, vol. 6, (4) 2016, pp. 1–17.

[11] W. Kwapil, J. Dalke, R. Post, T. Niewelt, Influence of dopant elements on degradation phenomena in B- and Ga-doped Czochralski-grown silicon, Solar RRL 5 (5) (2021) 2100147.

[12] N.E. Grant, P.P. Altermatt, T. Niewelt, R. Post, W. Kwapil, M.C. Schubert, J.D. Murphy, Gallium-doped silicon for high-efficiency commercial passivated emitter and rear solar cells, Solar RRL 5 (4) (2021) 2000754.

[13] Y. Acker, J. Simon, A. Herguth, Formation dynamics of BH and GaH-pairs in crystalline silicon during dark annealing, Phys. Status Solidi a 219 (17) (2022) 2200142.

[14] K. Kutsukake, N. Usami, Y. Ohno, Y. Tokumoto, I. Yonenaga, Control of grain boundary propagation in mono-like Si: Utilization of functional grain boundaries, Appl. Phys. Express 6 (2) (2013) 025505.

[15] F. Maischner, S. Maus, J. Greulich, S. Lohmüller, E. Lohmüller, P. Saint-Cast, D. Ourinson, H. Vahlman, K. Hergert, S. Riepe, S. Glunz, S. Rein, LeTID mitigation via an adapted firing process in p-type PERC cells from SMART cast-monocrystalline, Czochralski and high-performance multicrystalline silicon, Prog. Photovolt., Res. Appl. 30 (2) (2022) 123–131.

[16] F. Maischner, J. Greulich, W. Kwapil, D. Ourinson, S. Glunz, S. Rein, LeTID Mitigation via an Adapted Firing Process in p-Type PERC Cells from Gallium-doped Czochralski Silicon, 2023, in preparation.

[17] F. Kersten, F. Fertig, K. Petter, B. Klöter, E. Herzog, M.B. Strobel, J. Heitmann, J.W. Müller, System performance loss due to LeTID, Energy Procedia 124 (2017) 540–546.

[18] J.A. Giesecke, M.C. Schubert, D. Walter, W. Warta, Minority carrier lifetime in silicon wafers from quasi-steady-state photoluminescence, Appl. Phys. Lett. 97 (9) (2010).

[19] P. Hamer, D. Chen, R.S. Bonilla, Thermal processes and their impact on surface-related degradation, Phys. Status Solidi (RRL) 16 (2) (2022) 2100464.

[20] D. Sperber, A. Graf, A. Heilemann, A. Herguth, G. Hahn, Bulk and surface instabilities in boron doped float-zone samples during light induced degradation treatments, Energy Procedia 124 (2017) 794–798.

[21] K. Kim, R. Chen, D. Chen, P. Hamer, A. Ciesla nee Wenham, S. Wenham, Z. Hameiri, Degradation of surface passivation and bulk in p-type monocrystalline silicon wafers at elevated temperature, IEEE J. Photovolt. 9 (1) (2019) 97–105.

[22] C. Sen, P. Hamer, A. Soeriyadi, B. Wright, M. Wright, A. Samadi, D. Chen, B.V. Stefani, D. Zhang, J. Wu, F. Jiang, B. Hallam, M. Abbott, Impact of surface doping profile and passivation layers on surface-related degradation in silicon PERC solar cells, Sol. Energy Mater. Sol. Cells 235 (2022) 111497.

[23] F. Chen, I. Romijn, A. Weeber, J. Tan, B. Hallam, J. Cotter, Relationship between PECVD silicon nitride film composition and surface and edge passivation, in: Proceedings of the 22nd European Photovoltaic Solar Energy Conference and Exhibition, 2007, pp. 1053–1060.

[24] A. Schmid, C. Fischer, D. Skorka, A. Herguth, C. Winter, A. Zuschlag, G. Hahn, On the role of AlO_x thickness in AlO_x/SiN_y: H layer stacks regarding light- and elevated temperature-induced degradation and hydrogen diffusion in c-Si, IEEE J. Photovolt. 11 (4) (2021) 967–973.

[25] U. Varshney, B. Hallam, P. Hamer, A. Ciesla, D. Chen, S. Liu, C. Sen, A. Samadi, M. Abbott, C. Chan, B. Hoex, Controlling light- and elevated-temperature-induced degradation with thin film barrier layers, IEEE J. Photovolt. 10 (1) (2020) 19–27.

[26] E. Urrejola, J. Hong, C. Charpentier, A. Zauner, S. Pouliquen, A. Madec, Dielectric capping layers for high efficiency rear passivated silicon solar cells, in: Proceedings of the 29th European Photovoltaic Solar Energy Conference and Exhibition, EU PVSEC, Amsterdam, the Netherlands, 2014, pp. 22–26.

[27] J.M. Fritz, A. Zuschlag, D. Skorka, A. Schmid, G. Hahn, Temperature dependent degradation and regeneration of differently doped mc-Si materials, Energy Procedia 124 (2017) 718–725.

[28] D. Chen, M. Vaqueiro Contreras, A. Ciesla, P. Hamer, B. Hallam, M. Abbott, C. Chan, Progress in the understanding of light- and elevated temperature-induced degradation in silicon solar cells: A review, Prog. Photovolt., Res. Appl. 29 (11) (2021) 1180–1201.